

Heavy flavor in relativistic heavy-ion collisions

E. L. Bratkovskaya^{1,2}, T. Song^{1,2}, H. Berrehrah^{1,2}, D. Cabrera^{1,2},
J. M. Torres-Rincon³, L. Tolos^{2,4}, W. Cassing⁵

¹ Institute for Theoretical Physics, JWG Universität, Frankfurt/M, Germany

² Frankfurt Institute for Advanced Studies, JWG Universität, Frankfurt/M, Germany

³ Subatech, UMR 6457, IN2P3/CNRS, Université de Nantes, École des Mines de Nantes

⁴ Institut de Ciències de l'Espai (IEEC/CSIC), Campus Univ. Autònoma de Barcelona, Spain

⁵ Institut für Theoretische Physik, Universität Gießen, Germany

E-mail: Elena.Bratkovskaya@th.physik.uni-frankfurt.de

Abstract. We study charm production in ultra-relativistic heavy-ion collisions by using the Parton-Hadron-String Dynamics (PHSD) transport approach. The initial charm quarks are produced by the PYTHIA event generator tuned to fit the transverse momentum spectrum and rapidity distribution of charm quarks from Fixed-Order Next-to-Leading Logarithm (FONLL) calculations. The produced charm quarks scatter in the quark-gluon plasma (QGP) with the off-shell partons whose masses and widths are given by the Dynamical Quasi-Particle Model (DQPM), which reproduces the lattice QCD equation-of-state in thermal equilibrium. The relevant cross sections are calculated in a consistent way by employing the effective propagators and couplings from the DQPM. Close to the critical energy density of the phase transition, the charm quarks are hadronized into D mesons through coalescence and/or fragmentation. The hadronized D mesons then interact with the various hadrons in the hadronic phase with cross sections calculated in an effective lagrangian approach with heavy-quark spin symmetry. The nuclear modification factor R_{AA} and the elliptic flow v_2 of D^0 mesons from PHSD are compared with the experimental data from the STAR Collaboration for Au+Au collisions at $\sqrt{s_{NN}}=200$ GeV and to the ALICE data for Pb+Pb collisions at $\sqrt{s_{NN}}=2.76$ TeV. We find that in the PHSD the energy loss of D mesons at high p_T can be dominantly attributed to partonic scattering while the actual shape of R_{AA} versus p_T reflects the heavy-quark hadronization scenario, i.e. coalescence versus fragmentation. Also the hadronic rescattering is important for the R_{AA} at low p_T and enhances the D -meson elliptic flow v_2 .

1. Introduction

The Quantum Chromo Dynamics (QCD) [1, 2, 3, 4] predicts that matter changes its phase at high temperature and density and bound (colorless) hadrons dissolve to interacting (colored) quarks and gluons, i.e. to the Quark-Gluon-Plasma (QGP). Such extreme conditions have existed in the early expansion of the universe and now can be realized in the laboratory by collisions of heavy-ions at ultra-relativistic energies. The study of the phase boundary and the properties of the QGP are the main goal of several present and future heavy-ion experiments at SPS (Super Proton Synchrotron), RHIC (Relativistic Heavy-Ion Collider), LHC (Large Hadron Collider) and the future FAIR (Facility for Antiproton and Ion Research) and NICA (Nuclotron-based Ion Collider fAcility) [5]. Since the QGP is created only for a short time (of a couple of fm/c) it is quite challenging to study its properties and to find the most sensible probes. The advantage of 'hard probes' such as mesons containing heavy quarks (charm and beauty) is, firstly, that

due to the heavy masses they are dominantly produced in the very early stages of the reactions with large energy-momentum transfer, contrary to the light hadrons and electromagnetic probes. Secondly, they are not in an equilibrium with the surrounding matter due to smaller interaction cross sections relative to the light quarks and, thus, may provide an information on their creation mechanisms. Moreover, due to the hard scale, perturbative QCD (pQCD) should be applicable for the calculation of heavy quark production. As shown in Ref. [6], the FONLL calculations are in good agreement with the experimental observables on charm meson spectra in p+p collisions. This provides a solid reference frame for studying the heavy-meson production and their flow pattern in heavy-ion collisions.

The first charm measurements at RHIC energies by the PHENIX[7] and STAR [8] collaborations were related to the single non-photonic electrons emitted from the decay of charm mesons. However, recently the STAR Collaboration measured directly the nuclear modification factor and the elliptic flow of D^0 mesons in Au+Au collisions at $\sqrt{s_{NN}}=200$ GeV [9, 10] which allows for a straightforward comparison with the theoretical model calculations. It has been observed that the R_{AA} and v_2 of charm mesons show a similar behavior as in case of light hadrons contrary to expectations from pQCD. Similar observations have been made at LHC energies, too [11].

It still remains a challenge for the theory to reproduce the experimental data and to explain simultaneously the large energy loss of charm quarks (R_{AA}) and the strong collectivity (v_2) (cf. e.g. [12, 13, 14, 16]). Commonly, the interactions of charm quarks with the partonic medium are based on pQCD with massless light quarks and a fixed or running coupling. However, lattice QCD and quasiparticle approaches lead to the notion of massive degrees-of-freedom with finite spectral width [15]. In this case the pQCD cross sections are no longer meaningful. Moreover, the conclusions on the amount of suppression due to collisional energy loss by means of the elastic interactions of charm quarks with the QGP partons versus the radiative energy loss due to the emission of soft gluons (i.e. gluon bremsstrahlung) are still far from being robust. Also the influence of hadronization and especially hadronic rescattering is not yet settled, too.

Our goal here is to study the charm dynamics based on a consistent microscopic transport approach for the charm production, hadronization and rescattering with the partonic and hadronic medium. In this study we will confront our calculations within the Parton-Hadron-String Dynamics (PHSD) approach to the experimental data on charm at RHIC and LHC energies and discuss the perspectives/problems of using the charm quarks for the tomography of the QGP. To achieve this goal we embed the heavy-quark physics in the existing PHSD transport approach [17] which incorporates explicit partonic degrees-of-freedom in terms of strongly interacting quasiparticles (quarks and gluons) in line with an equation-of-state from lattice QCD (lQCD) as well as dynamical hadronization and hadronic elastic and inelastic collisions in the final reaction phase. Since PHSD has been successfully applied to describe the final distribution of mesons (with light quark content) from lower SPS up to LHC energies [17, 18, 19, 20], it provides a solid framework for the description of the creation, expansion and hadronization of the QGP as well as the hadronic expansion with which the heavy quarks interact either as quarks or as bound states such as D -mesons. We note in passing that in the hadronic phase PHSD merges with the familiar Hadron-String-Dynamics (HSD) approach [21, 22].

2. Description of charm production and dynamics in PHSD

2.1. Charm production in p+p collisions

Before studying the charm production in relativistic heavy-ion collisions, we discuss the charm production in p+p collisions at the top RHIC energy of $\sqrt{s_{NN}} = 200$ GeV. The charm production in p+p collisions also plays the role as a reference for the nuclear modification factor R_{AA} in heavy-ion collisions.

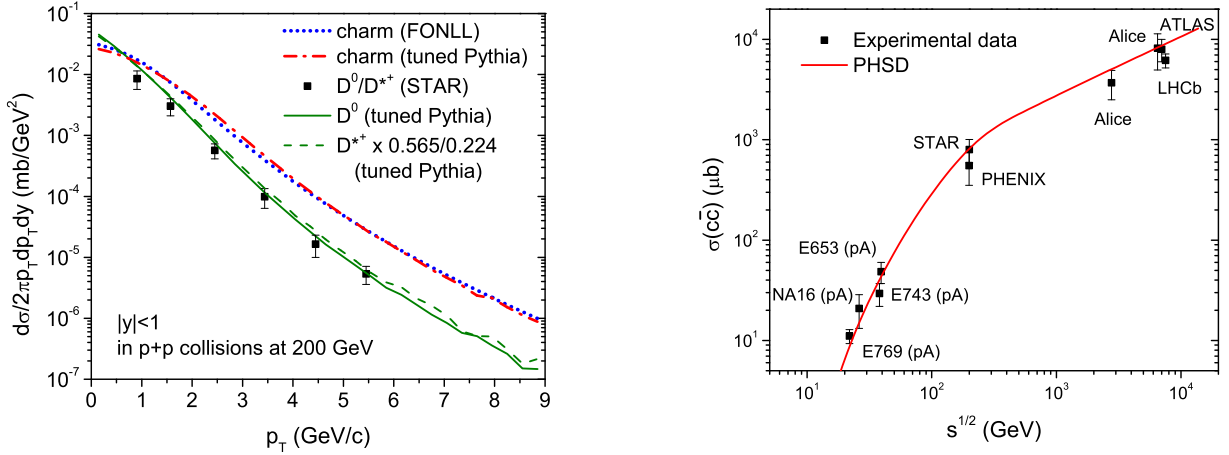


Figure 1. (l.h.s.) Transverse momentum distributions (upper lines) of charm quarks in p+p collisions at $\sqrt{s_{NN}}=200$ GeV from FONLL (dotted lines) and the tuned Pythia event generator (dot-dashed lines); in the lower lines the transverse momentum spectrum of D^0 mesons – which are fragmented from charm quarks with the contribution from D^* decay included (solid line) – and that of D^{*+} after scaling are compared with the experimental data from the STAR Collaboration [24]. (r.h.s.) The total cross section for charm production in p+p collisions (as parameterized in the PHSD) in comparison with the experimental data at various collision energies [24, 25].

We use the Pythia event generator to produce charm and anticharm quarks in p+p collisions with the parameters $PARP(91)=1.0$ GeV/c and $PARP(67)=1.0$ as in Ref. [23]. The former parameter is the Gaussian width of the primordial transverse momentum of a parton which initiates a shower in hadrons and the latter the parton shower level parameter. We note that by an additional suppression of the transverse momenta of charm and anticharm quarks by 10 % and a suppression of rapidities by 16 % the transverse momentum spectrum as well as rapidity distribution of charm and anticharm quarks from the Pythia event generator are very similar to those from the FONLL calculations in p+p collisions at $\sqrt{s_{NN}}=200$ GeV as shown in Fig. 1 (l.h.s.). Here the red dot-dashed lines are from the Pythia event generator (after tuning) and the blue dotted lines from the FONLL calculations, respectively.

The produced charm and anticharm quarks hadronize by emitting soft gluons. The probabilities for a charm quark to hadronize into D^0 , D^+ , D^{*0} , D^{*+} , D_s^+ , and Λ_c are, respectively, are specified in Ref. [23] together with the fragmentation function. The solid line in Fig. 1 (l.h.s.) shows the transverse momentum spectrum of D^0 mesons after charm quark fragmentation including the contribution from the decay of D^{*0} and D^{*+} . We can see that our results reproduce the experimental data from the STAR Collaboration [24] reasonably well.

Since charm-quark production requires a high energy-momentum transfer, the number of produced charm quark pairs in relativistic heavy-ion collisions is proportional to the number of binary nucleon-nucleon collisions N_{bin} . Since the probability to produce a charm quark pair depends on invariant energy and is less than that for primary hard collision in the PHSD, the binary nucleon-nucleon collisions producing charm quark pairs in PHSD are chosen by Monte Carlo from the ratio of the cross section for charm production in nucleon-nucleon collisions, $\sigma_{cc}^{pp}(\sqrt{s})$, to the inelastic nucleon-nucleon cross section. The actual charm cross section $\sigma_{cc}^{pp}(\sqrt{s})$ (red solid line) is shown in Fig. 1 (r.h.s.) in comparison to the experimental data from [24, 25].

2.2. Heavy quark scattering in the QGP

Quarks, antiquarks, and gluons are dressed in the QGP and have temperature-dependent effective masses and widths. In the DQPM, the mass and width of the light partons are given by thermal quantum-field theory assuming leading order diagrams but the strong coupling $g^2(T)$ is fitted to lattice data on energy and entropy densities, etc. [15]. Note that a nonzero width of a parton reflects the off-shell nature as well as the strong interaction of the quasi-particle and finite life-time.

The charm and anticharm quarks produced in early hard collisions interact with the dressed off-shell partons in the QGP. The cross sections for the charm quark scattering with massive off-shell partons are calculated considering the mass spectra of final state particles [26, 27]. In the current study the charm quark mass is taken to be 1.5 GeV and its mass spectrum is neglected for simplicity.

In the present study we consider only elastic scattering of charm quarks by light quarks and gluons. We do not consider yet the radiative processes which generate radiative energy loss because we expect that, due to the large gluon mass in the DQPM, the radiative processes are sub-dominant as compared to the collisional ones, especially for low charm-quark momenta (p_T). We expect the radiative energy loss to contribute at very high p_T as accessible experimentally at the LHC [28].

We emphasize that the transport coefficient D_s for charm quark diffusion – extracted from our microscopic calculations – and its agreement with the IQCD results (within errors) and the corresponding D meson D_s in hadronic medium validate our description for the coupling of charm with the QGP matter [29].

2.3. Hadronization of charm quarks

Since the hot and dense matter created by a relativistic heavy-ion collision expands with time, the energy density of the matter decreases and the deconfined degrees-of-freedom hadronize to color neutral hadronic states. Once the local energy density in PHSD becomes lower than 0.5 GeV/fm³, the partons are hadronized. First we look for all combinations of a charm quark and light antiquarks or of an anticharm quark and a light quark and calculate the probability for each combination to form a D or D^* (or D_s, D_s^*) meson. The probability for a quark and an anti-quark to form a meson is given by

$$f(\vec{\rho}, \mathbf{k}_\rho) = \frac{8g_M}{6^2} \exp \left[-\frac{\vec{\rho}^2}{\delta^2} - \mathbf{k}_\rho^2 \delta^2 \right], \quad (1)$$

where g_M is the degeneracy of the meson M , and

$$\vec{\rho} = \frac{1}{\sqrt{2}}(\mathbf{r}_1 - \mathbf{r}_2), \quad \mathbf{k}_\rho = \sqrt{2} \frac{m_2 \mathbf{k}_1 - m_1 \mathbf{k}_2}{m_1 + m_2}, \quad (2)$$

with m_i , \mathbf{r}_i and \mathbf{k}_i being the mass, position and momentum of the quark or antiquark i , respectively. The width parameter δ is related to the root-mean-square radius of the meson produced through $\langle r^2 \rangle = 3(m_1^2 + m_2^2)/(2(m_1 + m_2)^2) \delta^2$ and thus determined by experiment (if available). However, we will use this radius as a free parameter and evaluate the coalescence for a D -meson radius of 0.5 and 0.9 fm (see below). For further details we refer the reader to [23].

Collecting all possible combinations of a charm or an anticharm quark with light quarks or antiquarks and calculating the coalescence probability for each combination from Eq. (1), we obtain the probability for the charm or the anticharm quark to hadronize by coalescence in the actual space-time volume $\Delta t \Delta x \Delta y \Delta z$. Whether the charm or the anticharm quark is actually hadronized by coalescence is decided by Monte Carlo. Once the charm or the anticharm quark is decided to be hadronized by coalescence, then we find its partner again by Monte Carlo

on the basis on the probability of each combination in the selected local ensemble. In case the charm or anticharm quark is decided not to hadronize by coalescence, it is hadronized by the fragmentation method as in p+p collisions (cf. Section 2.1). Since the hadronization by coalescence is absent in p+p collisions, it can be interpreted as a nuclear matter effect on the hadronization of charm and anticharm quarks.

2.4. *D meson scattering in the hadron gas*

The D and D^* mesons produced through coalescence or fragmentation interact with the surrounding hadrons in PHSD. The presence of several resonances close to threshold energies with dominant decay modes involving open-charm mesons and light hadrons suggests that the scattering cross sections of a D/D^* off a meson or baryon, highly abundant in the post-hadronization medium, could manifest a non-trivial energy, isospin and flavor dependence. An example of these states is the broad scalar resonance $D_0(2400)$, which decays into the pseudoscalar ground state D by emitting a pion in the s -wave (similarly to the heavy-quark spin partner $D_1(2420)$, decaying into $D^*\pi$). Moreover, the similarity between the $\Lambda(1405)$ and the $\Lambda_c(2595)$ has driven the attention to the fact that the latter could be playing the role of a sub-threshold resonance in the DN system, connected to the latter by coupled-channel dynamics.

All these features have been addressed within several recent approaches based on hadronic effective models which incorporate chiral symmetry breaking in the light sector. The additional freedom stemming from the coupling to heavy-flavored mesons is constrained by imposing heavy-quark spin symmetry (HQSS). Whereas chiral symmetry fully determines the scattering amplitudes of Goldstone bosons with other hadrons at leading order in a model independent way, by means of HQSS the dynamics of the pseudoscalar and the vector mesons containing heavy quarks can be connected, since all kinds of spin interactions are suppressed in the limit of infinite quark masses [30]. For further details we refer the reader to Ref. [23] and the original literature cited therein.

3. Comparison to experiment

We now turn to actual nucleus-nucleus collisions at RHIC and LHC energies. Here the nuclear modification of D mesons is expressed in term of the ratio R_{AA} which is defined as

$$R_{AA}(p_T) \equiv \frac{dN_D^{\text{Au+Au}}/dp_T}{N_{\text{binary}}^{\text{Au+Au}} \times dN_D^{\text{p+p}}/dp_T}, \quad (3)$$

where $N_D^{\text{Au+Au}}$ and $N_D^{\text{p+p}}$ are, respectively, the number of D mesons produced in Au+Au collisions and that in p+p collisions, and $N_{\text{binary}}^{\text{Au+Au}}$ is the number of binary nucleon-nucleon collisions in Au+Au (Pb+Pb) collisions for the centrality class considered. If the matter produced in relativistic heavy-ion collisions does not modify the D meson production and propagation, the numerator of Eq. (3) should be equal to the denominator. Therefore, an R_{AA} smaller or larger than one implies that the nuclear matter suppresses or enhances D mesons, respectively. The elliptic anisotropy in the azimuthal angle ψ is characterized by

$$v_2 = \langle \cos(2\psi - 2\Psi_{RP}) \rangle = \left\langle \frac{p_x^2 - p_y^2}{p_x^2 + p_y^2} \right\rangle, \quad (4)$$

where p_x and p_y are the x and y components of the particle momenta and Ψ_{RP} is the azimuth of the reaction plane while the brackets denote averaging over particles and events. The v_2 coefficient can be considered as a function of centrality, rapidity y and/or transverse momentum p_T . We note that the reaction plane in PHSD is given by the $(x-z)$ plane with the z -axis in the beam direction.

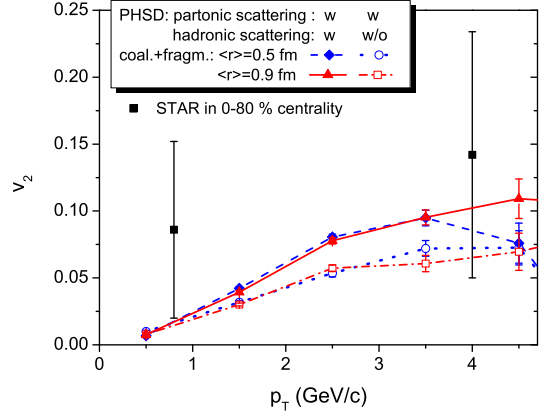
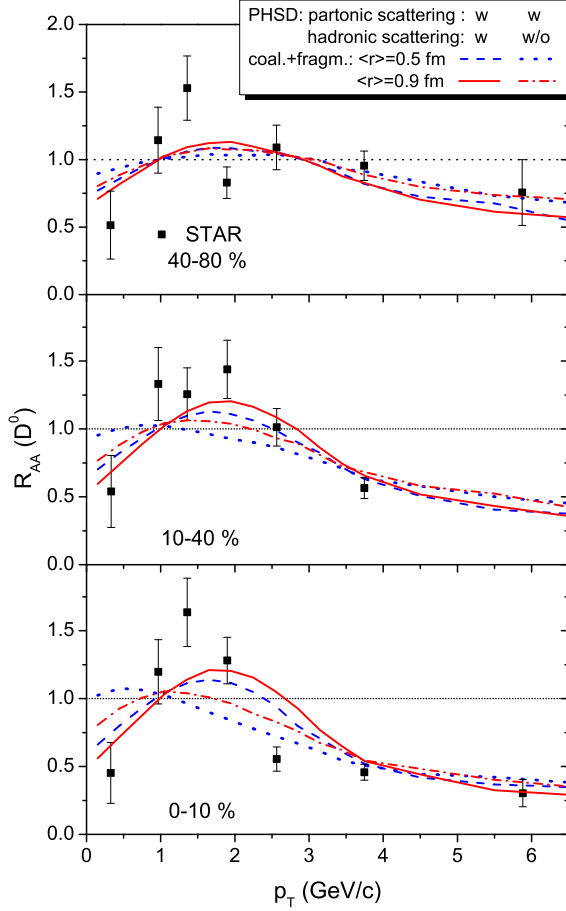


Figure 2. (l.h.s.) The R_{AA} of D^0 mesons including partonic scattering with (dashed and solid lines) and without hadronic scattering (dotted and dot-dashed lines) in Au+Au collisions at $\sqrt{s_{NN}} = 200$ GeV for a D meson radius of 0.5 fm and of 0.9 fm. The experimental data are from the STAR Collaboration [9, 10]. (r.h.s.) The elliptic flow v_2 of D^0 mesons including partonic scattering with (dashed and solid lines) and without hadronic scattering (dotted and dot-dashed lines) in Au+Au collisions at $\sqrt{s_{NN}} = 200$ GeV for a D meson radius of 0.5 fm and of 0.9 fm.

Fig. 2 shows the R_{AA} (l.h.s.) and the elliptic flow v_2 of D^0 mesons (r.h.s.) with and without hadronic scattering. We can see that the hadronic scattering plays an important role both in R_{AA} and the elliptic flow v_2 . It shifts the peak of R_{AA} to higher transverse momentum especially in central collisions and enhances the elliptic flow of final D mesons.

In Fig. 3 we present our *preliminary* results for the LHC energies. The left part of the figure shows the PHSD results for the R_{AA} of $D^0 + D^+ + D^{*+}$ mesons at midrapidity for 20% central Pb+Pb collisions at $\sqrt{s_{NN}} = 2.76$ TeV calculated without (red line) and with (blue line) shadowing [31] in comparison to the experimental data from the ALICE Collaboration [32]. As seen the shadowing effect reduces the peak at low p_T , which is still higher than the experimental data. The suppression of the high p_T tail is comparable with the corresponding results for RHIC energies and approximately in line with the data. We stress again that we did not account for radiative energy loss in the present calculations which might play a role at higher p_T [28].

The right part of figure 3 shows the corresponding v_2 for 20% central Pb+Pb collisions for the scenario including shadowing. We note that the v_2 -flow for central (0-20%) collisions is lower than that for semi-central (30-50%) measured by the ALICE Collaboration [33], however, still quite substantial (up to 10%) and comparable with the v_2 of light hadrons for the same centrality.

4. Summary

We have studied charm production in relativistic heavy-ion collisions by using the Parton-Hadron-String Dynamics (PHSD) approach [18] where the initial charm quark pairs are produced

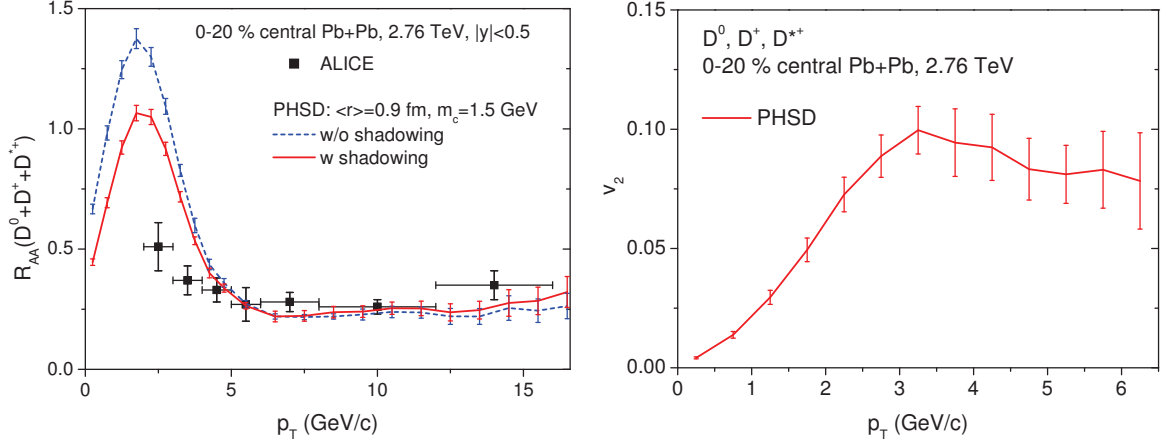


Figure 3. (l.h.s.) The PHSD results for the R_{AA} of $D^0 + D^+ + D^{*+}$ mesons at midrapidity for 0-20% central Pb+Pb collisions at $\sqrt{s_{NN}}=2.6$ TeV calculated without (dashed blue line) and with (solid red line) shadowing in comparison to the experimental data from the ALICE Collaboration [32]. (r.h.s.) The PHSD results for the v_2 versus p_T of $D^0 + D^+ + D^{*+}$ mesons for 20% central Pb+Pb collisions at $\sqrt{s_{NN}}=2.6$ TeV including the shadowing effect.

in binary nucleon-nucleon collisions from the PYTHIA event generator taking into account the smearing of the collision energy due to the Fermi motion of nucleons in the initial nuclei. The produced charm and anticharm quarks interact with the dressed quarks and gluons in the QGP which are described by the Dynamical Quasi-Particle Model [15] in PHSD. The interactions of the charm quarks with the QGP partons have been evaluated with the DQPM propagators and couplings consistently [26]. We mention that when extracting the spatial diffusion coefficient D_s from our cross sections as a function of the temperature we observe a minimum of D_s close to T_c which is in line with lattice data above T_c and hadronic many-body calculations below T_c (cf. Ref. [29]).

We have found that the interaction of the charm quarks with the dynamical partons of the QGP softens the p_T spectrum of charm and anticharm quarks but does not lead to a full thermalization for transverse momenta $p_T > 2$ GeV/c. The charm and anticharm quarks, furthermore, are hadronized to D mesons either through the coalescence with a light quark or antiquark or through the fragmentation by emitting soft 'perturbative' gluons. Since the hadronization through coalescence is absent in p+p collisions, it can be interpreted as a nuclear matter effect on the D meson production in relativistic heavy-ion collisions. In the coalescence mechanism the charm or anticharm quark gains momentum by fusing with a light quark or antiquark while it loses momentum in the fragmentation process (as in p+p reactions). This partly contributes to the large R_{AA} of D mesons between 1 and 2 GeV/c of transverse momentum. Finally, the formed D mesons interact with hadrons by using the cross sections calculated in an effective lagrangian approach with heavy quark spin-symmetry [30], which is state-of-the art. We have found that the contribution from hadronic scattering both to the R_{AA} and to the elliptic flow of D mesons is appreciable, especially in central collisions, and produces additional elliptic flow v_2 [23].

Since the PHSD results reproduce the experimental data from the STAR and ALICE Collaborations without radiative energy loss in the p_T range considered, we conclude that collisional energy loss is dominant at least up to $p_T = 6$ (15) GeV/c in relativistic heavy-ion collisions at RHIC (LHC). In our approach this is essentially due to the infrared enhanced coupling $\alpha_s(T)$ in the DQPM leading to large scattering cross sections of charm quarks with partons at temperatures close to T_c .

Acknowledgements

The authors acknowledge inspiring discussions with J. Aichelin, P. B. Gossiaux, C. M. Ko, O. Linnyk, R. Marty, V. Ozvenchuk, and R. Vogt. This work was supported by DFG under contract BR 4000/3-1, and by the LOEWE center "HIC for FAIR". JMTR is supported by the Program TOGETHER from Region Pays de la Loire and the European I3-Hadron Physics program. LT acknowledges support from the Ramon y Cajal Research Programme and contracts FPA2010-16963 and FPA2013-43425-P from Ministerio de Ciencia e Innovación, as well as from FP7-PEOPLE-2011-CIG under Contract No. PCIG09-GA-2011-291679. The computational resources have been provided by the LOEWE-CSC.

References

- [1] Aoki Y *et al.* 2006 *Phys. Lett. B* **643** 46
- [2] Borsanyi S *et al.* 2010 *JHEP* **1009** 073; 2010 *JHEP* **1011** 077; 2012 *JHEP* **1208** 126; 2014 *Phys. Lett. B* **730** 99; 2015 *Phys. Rev. D* **92** 014505
- [3] Petreczky P [HotQCD Collaboration] 2012 *PoS LATTICE* **2012** 069
- [4] Ding H-T Karsch F Mukherjee S 2015 arXiv:1504.05274
- [5] Proceedings of Quark Matter-2014 2014 *Nucl. Phys. A* **931** 1
- [6] Cacciari M Nason P Vogt R 2005 *Phys. Rev. Lett.* **95** 122001
- [7] Adare A *et al.* (PHENIX Collaboration) 2007 *Phys. Rev. Lett.* **98** 172301
- [8] Abelev B I *et al.* [STAR Collaboration] 2007 *Phys. Rev. Lett.* **98** 192301
- [9] Adamczyk L *et al.* [STAR Collaboration] 2014 *Phys. Rev. Lett.* **113** 142301
- [10] Thusty D [STAR Collaboration] 2013 *Nucl. Phys. A* **904-905** 639c
- [11] Sakai S *et al.* 2013 *Nucl. Phys. A* **904-905** 661c
- [12] van Hees H Greco V and Rapp R 2006 *Phys. Rev. C* **73** 034913
- [13] Uphoff J *et al.* 2013 *Nucl. Phys. A* **910-911** 401; *ibid* 2014 **931** 535.
- [14] Das S K Scardina F Plumari S Greco V 2014 *Phys. Rev. C* **90** 044901
- [15] Cassing W 2009 *Eur. Phys. J. ST* **168** 3; 2007 *Nucl. Phys. A* **795** 70
- [16] Ozvenchuk V *et al.* 2014 *Phys. Rev. C* **90** 054909
- [17] Cassing W Bratkovskaya E L 2009 *Nucl. Phys. A* **831** 215
- [18] Bratkovskaya E L Cassing W Konchakovski V P Linnyk O 2011 *Nucl. Phys. A* **856** 162
- [19] Konchakovski V P *et al.* 2015 *J. Phys. G* **42** 055106; 2014 *J. Phys. G* **41** 105004; 2014 *Phys. Rev. C* **90** 014903; 2012 *Phys. Rev. C* **85** 044922; 2012 *Phys. Rev. C* **85** 011902
- [20] Linnyk O *et al.* 2014 *Phys. Rev. C* **89** 034908; 2013 *Phys. Rev. C* **88** 034904; 2013 *Phys. Rev. C* **87** 014905; 2012 *Phys. Rev. C* **85** 024910; 2011 *Phys. Rev. C* **84** 054917; 2011 *Nucl. Phys. A* **855** 273
- [21] Cassing W Bratkovskaya E L 1999 *Phys. Rep.* **308** 65
- [22] Cassing W Bratkovskaya E L Juchem S 2000 *Nucl. Phys. A* **674** 249
- [23] Song T Berrehrah H Cabrera D Torres-Rincon J M Tolos L Cassing W Bratkovskaya E L 2015 *Phys. Rev. C* **92** 014910
- [24] Adamczyk L *et al.* [STAR Collaboration] 2012 *Phys. Rev. D* **86** 072013
- [25] Conesa del Valle Z [ALICE Collaboration] 2012 *AIP Conf. Proc.* **1441** 886
- [26] Berrehrah H *et al.* 2014 *Phys. Rev. C* **89** 054901
- [27] Berrehrah H *et al.* 2014 *Phys. Rev. C* **90** 064906
- [28] Younus M Coleman-Smith C E Bass S A Srivastava D K 2015 *Phys. Rev. C* **91** 024912
- [29] Berrehrah H *et al.* 2014 *Phys. Rev. C* **90** 051901
- [30] Tolos L Torres-Rincon J M 2013 *Phys. Rev. D* **88** 074019
- [31] Eskola K J Paukkunen H Salgado C A 2009 *JHEP* **0904** 065
- [32] Abelev B *et al.* [ALICE Collaboration] 2012 *JHEP* **1209** 112
- [33] Abelev B *et al.* [ALICE Collaboration] 2013 *Phys. Rev. Lett.* **111** 102301

